EUROPEAN ORGANIZATION FOR NUCLEAR RESEARCH

CERN-PPE/94-73
9 May, 1994

Status of Higgs Hunting at the Z Resonance and its Prospects at LEP2

André Sopczak

PPE Division, CERN, CH-1211 Geneva 23

Abstract

Results from general searches for the Higgs boson of the Minimal Standard Model (MSM), and for neutral and charged Higgs bosons of non-minimal Higgs models are reviewed from the four LEP experiments at CERN: ALEPH, DELPHI, L3, and OPAL. A total of about 6 million hadronic Z decays have been analyzed during data-taking from 1989 to 1993. The Higgs boson discovery potential for LEP2 is presented, and requirements for a decisive test of the Minimal Supersymmetric Standard Model (MSSM) are discussed.

CERN PPE Seminar and talk given at the Lisbon Fall School 1993, to be published in the proceedings.

Status of Higgs Hunting at the Z Resonance and its Prospects at LEP2

André Sopczak[a]*

[a]PPE Division, CERN, CH-1211 Geneva 23

Results from general searches for the Higgs boson of the Minimal Standard Model (MSM), and for neutral and charged Higgs bosons of non-minimal Higgs models are reviewed from the four LEP experiments at CERN: ALEPH, DELPHI, L3, and OPAL. A total of about 6 million hadronic Z decays have been analyzed during data-taking from 1989 to 1993. The Higgs boson discovery potential for LEP2 is presented, and requirements for a decisive test of the Minimal Supersymmetric Standard Model (MSSM) are discussed.

1. Introduction

The search for Higgs particles [1] is one of the most challenging questions of experimental particle physics. Their discovery would confirm the mechanism used to generate masses in gauge theories and, more generally, the experimental evidence for Higgs bosons would be crucial to understand the mechanism of the $SU(2) \times U(1)$ symmetry breaking. The transition from LEP1 to LEP2 will result in an improved signal to background ratio for the Higgs search, as shown in Fig. 1.

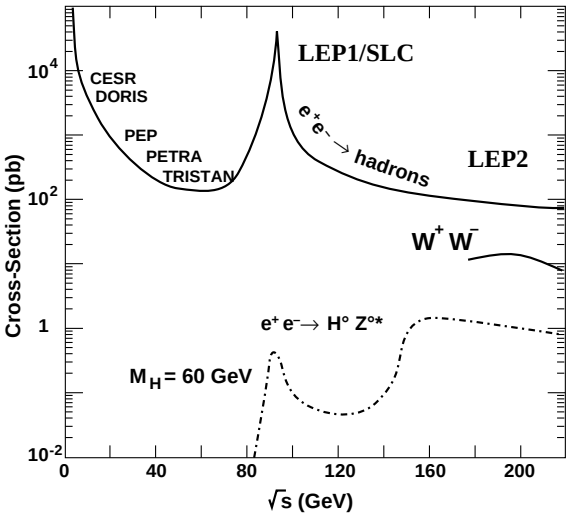

Figure 1. Background and signal cross sections as a function of the center-of-mass energy.

*e-mail: andre@cernvm.cern.ch

The Higgs mass is a free parameter in the Standard Model [2]. Current precision measurements of the Z-lineshape do not reveal a favored Higgs mass range, as illustrated in Fig. 2 (from [3]).

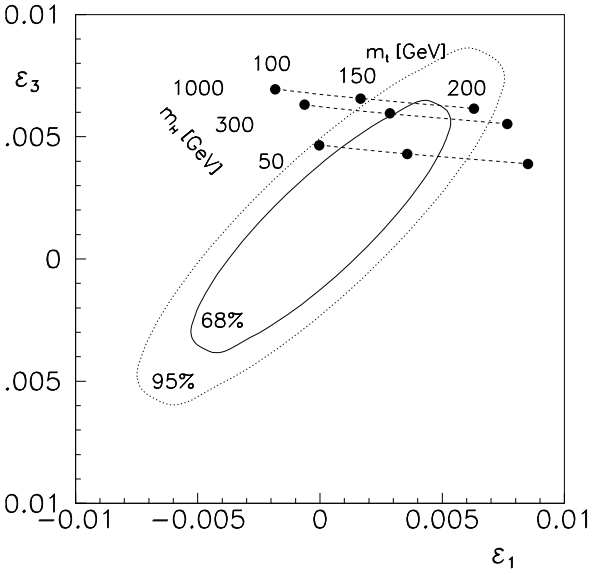

Figure 2. Comparison of Z-lineshape measurements with top and Higgs mass variations in the MSM.

The theoretical framework is reviewed, for example, in [4]. This paper reviews the search for the MSM Higgs (Sec. 2), and the search for non-minimal Higgs bosons (Sec. 3). Interpretations in the two-doublet Higgs model (Sec. 4), and in the MSSM (Sec. 5) are summarized. The physics potential for the extension to LEP2 energies around 200 GeV is addressed in Sec. 6.

2. MSM Higgs Search

The expected Higgs boson event rate [5] for the bremsstrahlung process [6] is known better than 1% including radiative corrections [7]. The expected number of Higgs boson events per 1 million hadronic Z decays is shown in Fig. 3.

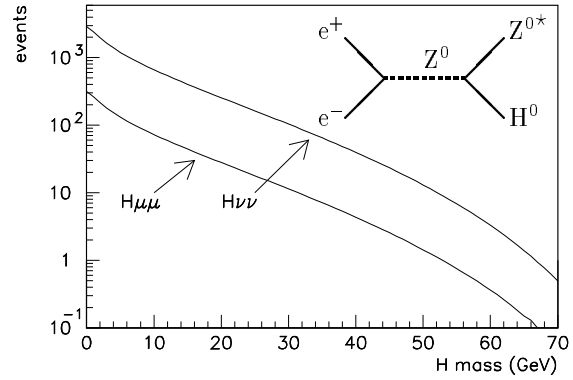

Figure 3. MSM Higgs production rate.

The Higgs decay mode determines the Higgs signature in the detectors. Higgs bosons with low masses decay into e^+e^- and $\mu^+\mu^-$ pairs, and for high masses the Higgs boson decays predominantly into a $b\bar{b}$ quark. Various other decay modes are possible, as shown in Fig. 4 (from [8]).

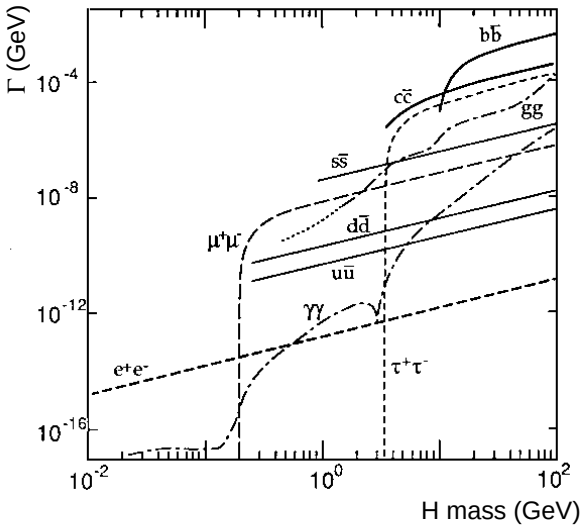

Figure 4. MSM Higgs decay branching ratios.

2.1. Very Low-Mass Higgs Bosons

For $m_{\rm H} < 2m_\mu$ the Higgs boson has a decay length such that it does not decay at the primary interaction point. Two signatures can be distinguished, a) the Higgs decays outside the detector, and b) the Higgs decays inside the detector material, leaving a 'V' signature. Figure 5 (from [8]) shows the decay length.

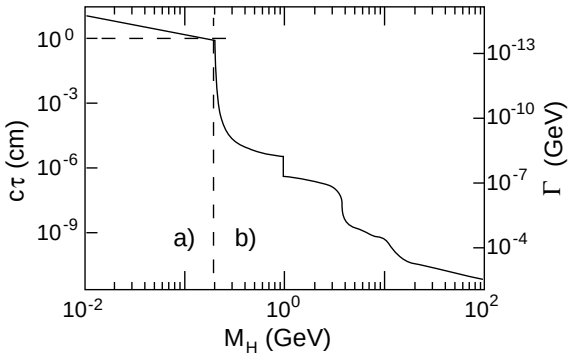

Figure 5. MSM Higgs decay length.

Searches for these signatures have been performed by all LEP experiments, and no indication of a signal has been observed. An example of the number of expected Higgs events is given in Fig. 6 (from[9]).

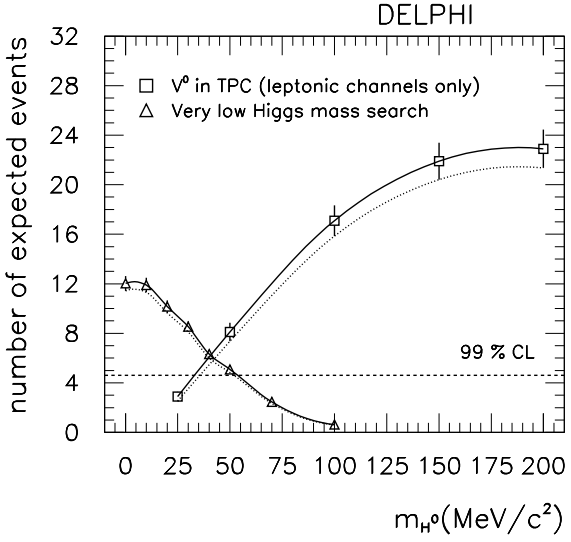

Figure 6. DELPHI: Number of expected Higgs events in the low-mass region.

2.2. Low-Mass Higgs Bosons

Various different final states are expected as illustrated in Fig. 7. No indication of a Higgs signal in any channel has been found, and the mass region below 4 GeV is excluded at 99% CL [10–13].

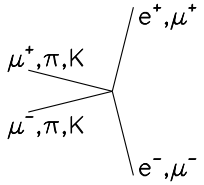

Figure 7. Diagrammatic view of a low-mass Higgs signal.

2.3. Intermediate-Mass Higgs Bosons

Mono-jets are expected in this mass region between about 4 and 15 GeV. Such mono-jets, as illustrated in Fig. 8, have not been observed and the mass region is excluded at 99% CL [10–13].

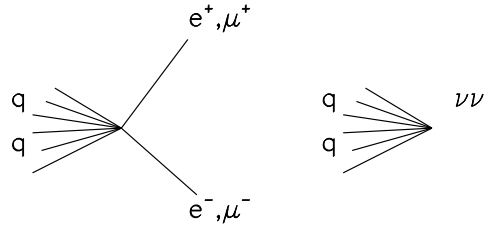

Figure 8. Diagrammatic view of an intermediate-mass Higgs signal.

2.4. High-Mass Higgs Bosons

In this mass region the muon, electron, and neutrino channels are very important. Typical Higgs signatures are illustrated in Fig. 9.

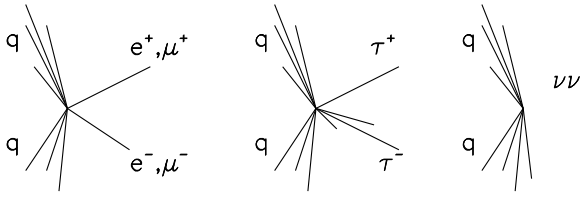

Figure 9. Diagrammatic view of a high-mass Higgs signal.

Figure 10 (from[13]) shows a $Z^{0\star}H^0 \to \mu^+\mu^- q\overline{q}$ candidate event which has passed all of the selection criteria, and Fig. 11 (from[12]) shows a $Z^{0\star}H^0 \to e^+e^- q\overline{q}$ candidate.

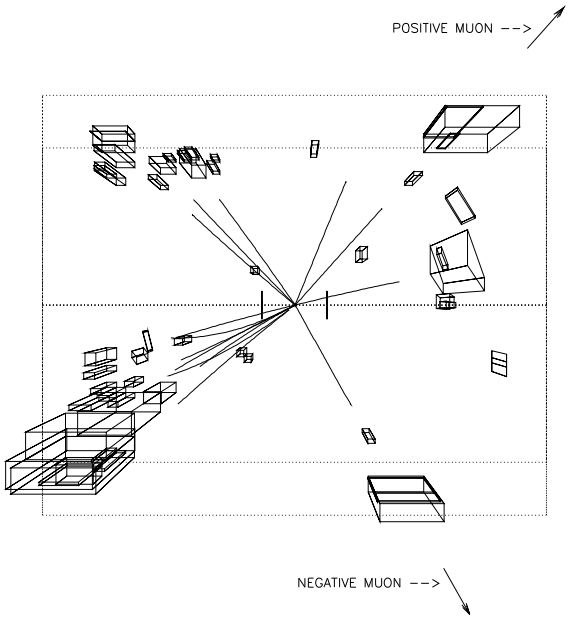

Figure 10. OPAL:Higgs candidate m_{H}=62.2GeV.

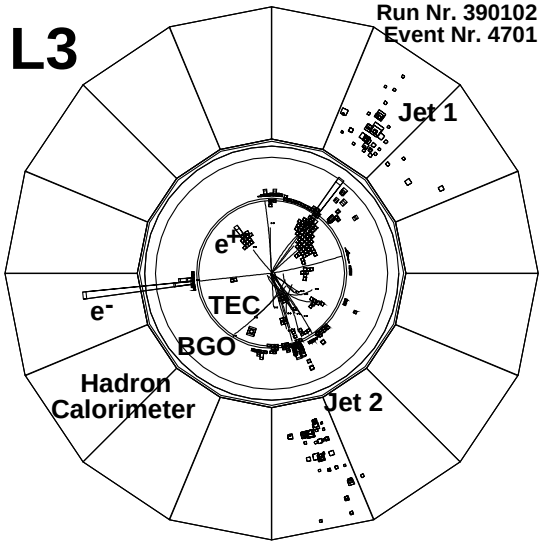

Figure 11. L3: Higgs candidate $m_{\mathrm{H}} = 67.6$ GeV.

Table 1 lists the Higgs candidates [10–13] with $m_{\mathrm{H}} > 30$ GeV. In the e^+e^- and $\mu^+\mu^-$ channels the precise measurement of the recoiling lepton mass corresponds to the Higgs boson mass.

Table 1
MSM Higgs Candidates.

Experiment	Event Type	Mass (GeV)
ALEPH	$\mu^+\mu^-q\bar{q}$	51.4 ± 0.5
OPAL	$\mu^+\mu^-q\bar{q}$	61.2 ± 1.0
L3	$e^+e^-q\bar{q}$	31.4 ± 1.5
	$\mu^+\mu^-q\bar{q}$	70.4 ± 0.7
	$e^+e^-q\bar{q}$	67.6 ± 0.7
DELPHI	$e^+e^-q\bar{q}$	35.9 ± 5.0

The remaining candidate events are well understood. They are a result of 4-fermion background. Their production graphs are shown in Fig. 12. Annihilation and conversion processes contribute mostly after all selection cuts for the Higgs signal are applied.

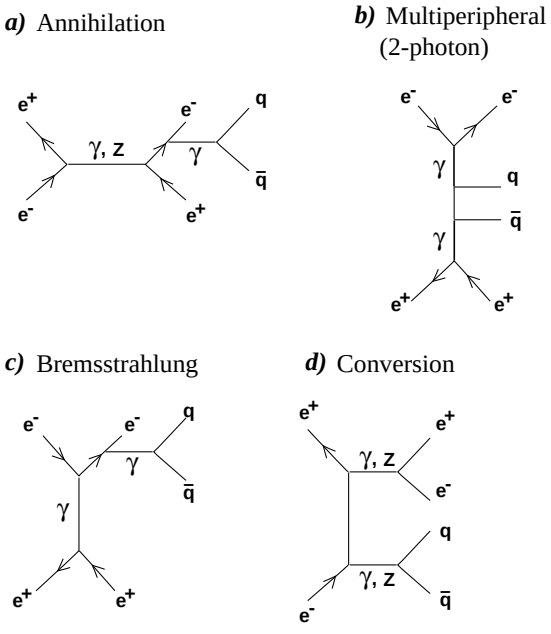

Figure 12. 4-fermion background reactions.

The spectrum of the recoiling mass, corresponding to the Higgs mass, is shown in Fig. 13 (from [10], preliminary) before a cut on this variable is applied. Two out of the three events in the mass region above 50 GeV are rejected since the jets are not likely to be b-flavored, as expected from a Higgs decay. The simulated 4-fermion spectrum is in full accordance with the data. For all four LEP experiments about nine 4-fermion events with recoiling mass > 50 GeV are expected, while four events have been observed. Table 2 summarizes the Higgs mass limits in the MSM [10–13].

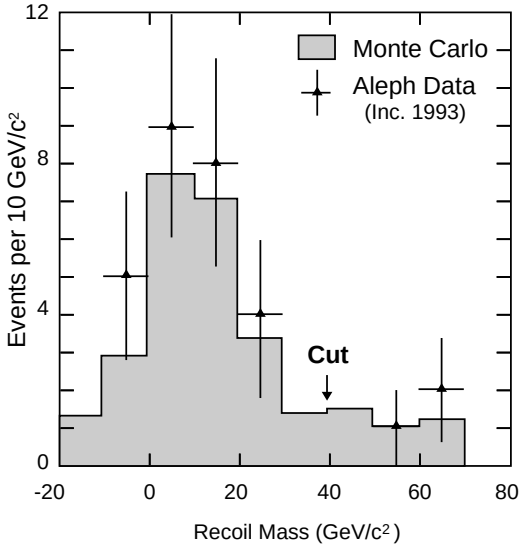

Figure 13. ALEPH: 4-fermion simulation and data.

Table 2
MSM Higgs boson mass limits from ALEPH, DELPHI, L3, and OPAL

	A Prel.	D Prel.	L3	O
Data Sample	89-93	90-92	90-92	90-93
$Z^0 \to q\bar{q} \times 10^6$	1.9	1.1	1.1	1.9
Sys. Err. (%)	2.0	3.0	2.6	2.4
Mass Limit				
95%CL (GeV)	**60.3**	**55.7**	**57.7**	**56.9**

The number of expected Higgs events are shown in Fig. 14 (from[12]) for the $\mu^+\mu^-$, e^+e^-, and $\nu\bar{\nu}$ channels. The limit is set using Poisson statistics. In a mass region without a Higgs candidate the 95% CL limit is set where the sum of the expected events is 3.

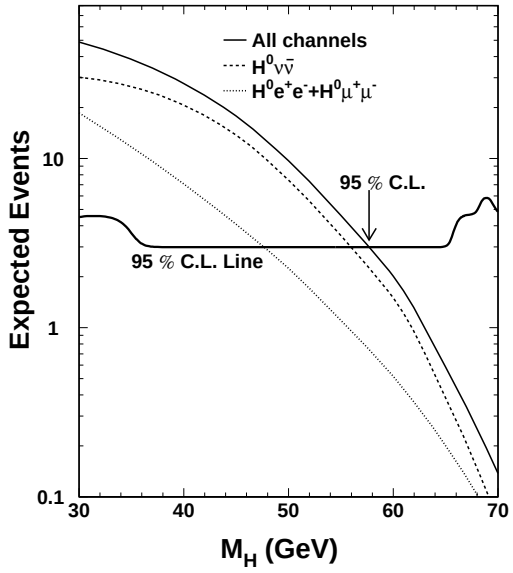

Figure 14. L3: Expected events in $\mu^+\mu^-$, e^+e^-, and $\nu\bar{\nu}$ channels, and the 95% CL line.

2.5. Combined Limit and Prospects

The number of expected events is given by each LEP experiment [10–13], and shown in Fig. 15 for published data corresponding to a total of 4.8 million hadronic Z decays. In first approximation, a combined Higgs mass limit can be set by the summation of the number of expected Higgs events.

The evolution of the published Higgs mass limits is shown in Fig. 16. The sensitivity can be extrapolated assuming 50% efficiency in the $\mu^+\mu^-$, e^+e^-, and $\nu\bar{\nu}$ channels. With about 10 million hadronic Z decays a sensitivity of 65 to 70 GeV could be obtained, depending on additional 4-fermion background events. The combined LEP limit lies below the extrapolated line, since all experiments have tuned the events selection on their own maximal visible Higgs mass.

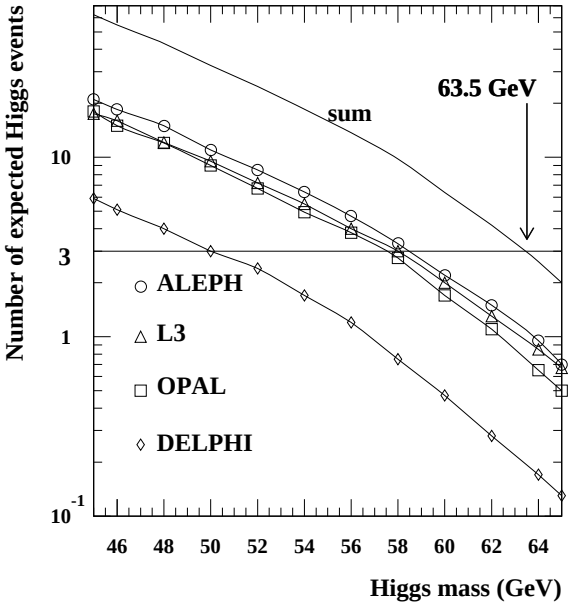

Figure 15. Combined mass limit from published ALEPH, DELPHI, L3, and OPAL results.

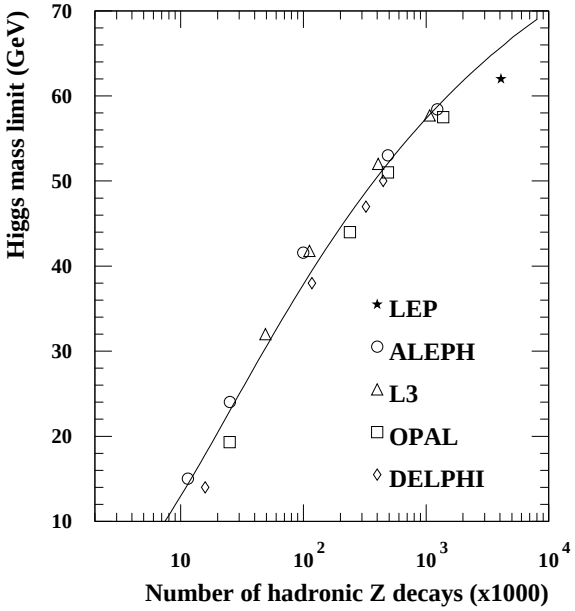

Figure 16. Published Higgs mass limits and extrapolation of sensitivity.

3. Non-Minimal Higgs Search

There are three classes of searches for non-minimal Higgs bosons: a) searches for Higgs bremsstrahlung with reduced production rates compared to the MSM prediction, b) neutral Higgs pair-production, and c) charged Higgs pair-production. The production graphs are shown in Fig. 17.

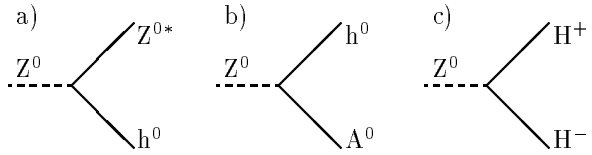

Figure 17. Non-minimal Higgs production.

3.1. Invisible Higgs Search

A heavy invisible Higgs boson can be searched in bremsstrahlung production as shown Fig 17 a) in analogy to the MSM Higgs boson. The electron, muon, and hadron channels are important. Larger sensitivities are expected compared to the MSM search, since the $Z^0 \to q\overline{q}$ channel gives a clean signature for the invisible Higgs. One invisible 60 GeV candidate event shown in Fig. 18 (from [14]) is compatible with the expected rate from the 4-fermion background.

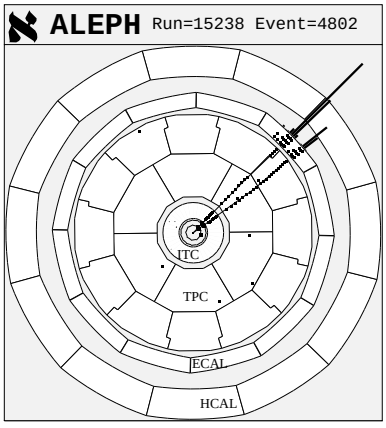

Figure 18. ALEPH: Invisible Higgs candidate in the electron channel.

Figure 19 (from [14]) shows limits at 95% CL normalized to the expected MSM Higgs rate: a) for MSM Higgs production, and b) for invisible Higgs production.

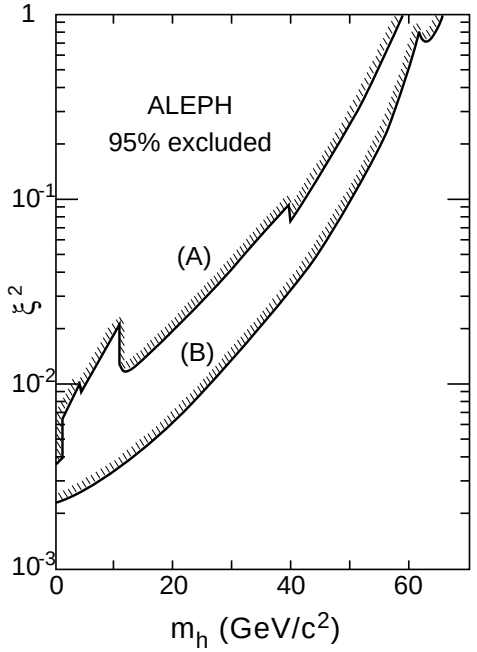

Figure 19. ALEPH: (A) MSM, and (B) invisible Higgs limits.

3.2. $Z^0 \to h^0A^0 \to b\bar{b}b\bar{b}$ Search

In this channel 4-jet events are expected. A good hadronic mass resolution would allow reconstruction of both Higgs masses and thus the combinatorial background from $Z^0 \to q\bar{q}$ can be reduced, as shown in Fig. 20 (from [15]).

Many 4-jet events pass the event-shape and invariant mass selection cuts. One simulated example of such an event is shown in Fig. 21 (from [16]) as expected from QCD processes (Fig. 22).

A further event selection is based on the fact that Higgs events produce b-flavored jets. These jets can be selected by semileptonic b-decays. Good purity is obtained by requiring large transverse momentum of the lepton with respect to the jet direction, as shown in Fig. 23 (from [17]).

All LEP experiments are equipped with microvertex detectors. B mesons have a long lifetime (τ_B = 1.3 ps) which gives a larger number of detectable secondary vertices. These detectors allow the tagging of b-flavored jets by tracking particles with high accuracy close to the interaction point. Figure 24 (from [18]) shows a bbbb candidate.

The limits on $\Gamma(Z^0 \to h^0 A^0)/\Gamma(Z^0 \to q\bar{q})$ vary with m_h and m_A. These limits are of the order of 10^{-3} with semi-leptonic tagging, and up to 10^{-4} with lifetime-tagging [14,11,15,19,18].

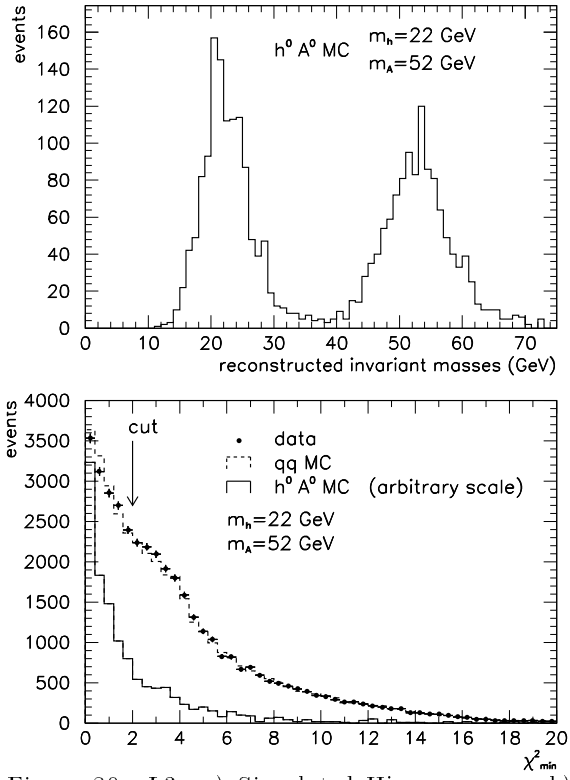

Figure 20. L3: a) Simulated Higgs masses. b) Mass-χ^2 for data, $q\overline{q}$ MC, and simulated signal.

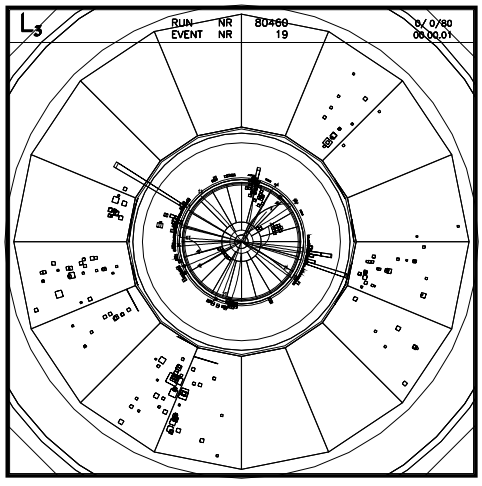

Figure 21. Simulated 4-jet event.

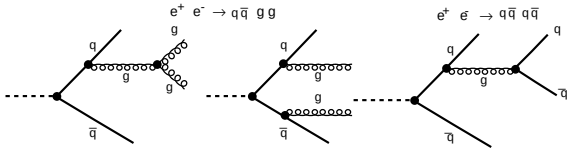

Figure 22. QCD Feynman graphs leading to 4-jet events.

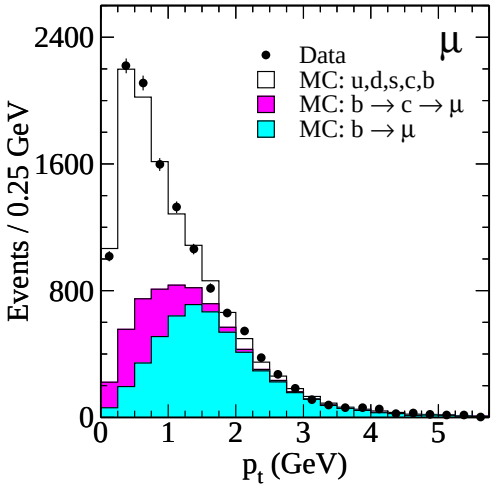

Figure 23. L3: b-jet tagging with semileptonic b-decays. Good b-jet purity is achieved for events with large transverse lepton momentum.

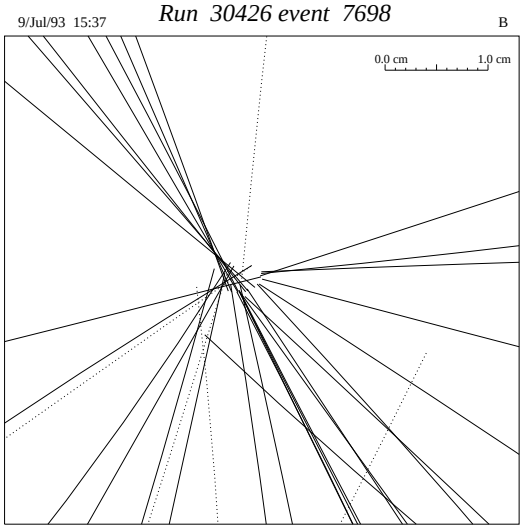

Figure 24. DELPHI: b-jet tagging using a microvertex detector. Tracks tend to cluster in different vertices.

3.3. $Z^0 \to h^0A^0 \to \tau^+\tau^-b\bar{b}$ Search

In this channel a τ-pair recoiling to a jet system is expected. The invariant mass of the τ-pair can be reconstructed using kinematic constraints. Figure 25 (from [15]) shows a simulated Higgs signal in comparison with data and background simulation, and below, branching ratio limits after scanning over all mass combinations.

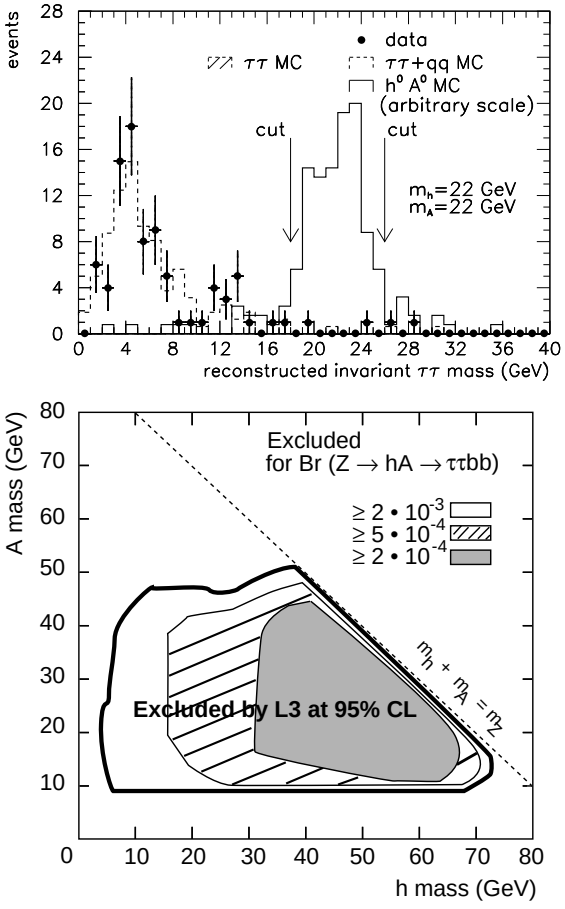

Figure 25. L3: Results in the $\tau\tau$bb channel.

3.4. $Z^0 \to h^0A^0 \to \tau^+\tau^-\tau^+\tau^-$ Search

Four τ-events have been searched for and no signal has been observed. The most important background originates from $Z^0 \to \tau^+\tau^-$ events. This background can be largely suppressed by requiring exactly two tracks in one hemisphere as expected from one-prong $h^0 \to \tau^+\tau^-$ decays, as shown in Fig. 26 (from [15]).

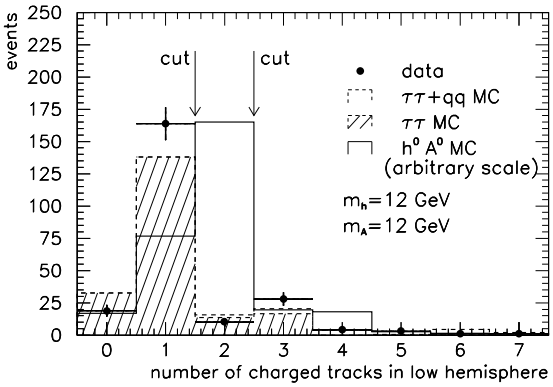

Figure 26. L3: Results in the $\tau\tau\tau\tau$ channel.

3.5. $h^0 \to A^0A^0$ Search

The $h^0 \to A^0A^0$ decay can be dominant if kinematically allowed. No indication of a Higgs has been observed and limits are set, for example, on six τ's or six b's of about 10^{-3} [14,11,15,19].

3.6. $Z^0 \to H^+H^- \to c\bar{s}\bar{c}s$ Search

Compared to the bbbb channel very similar signatures are expected. Furthermore, kinematic constraints can be applied, and a charged Higgs mass resolution better than 1 GeV is expected. However, b-tagging cannot be applied, and more irreducible background events remain as shown in Fig. 27 (from [15]).

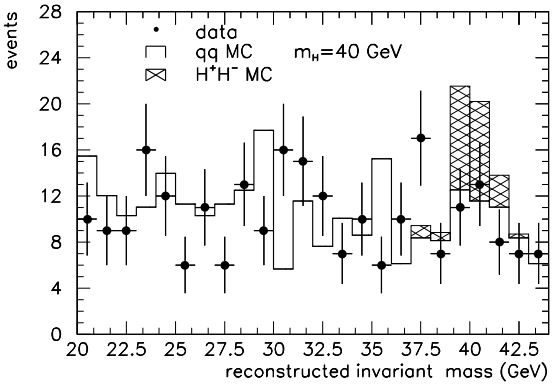

Figure 27. L3: Data, simulated background, and a 40 GeV cscs Higgs signal.

3.7. $Z^0 \to H^+H^- \to cs\tau\nu$ Search

After all selection cuts, a Higgs signal would be clearly visible in the reconstructed jet-jet invariant mass distribution, as shown in Fig. 28 (from [15]).

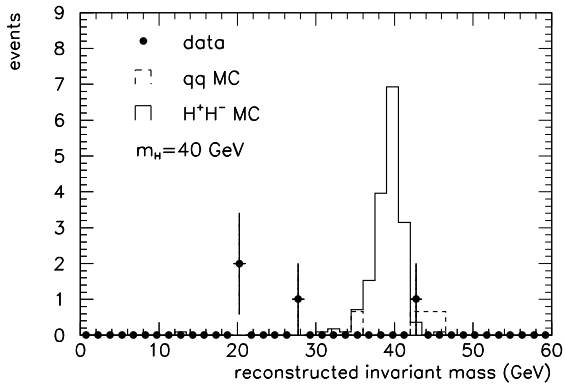

Figure 28. L3: Data, simulated background, and a 40 GeV cs$\tau\nu$ Higgs signal.

3.8. $Z^0 \to H^+H^- \to \tau^+\nu\tau^-\bar{\nu}$ Search

Figure 29 (from [15]) shows a good separation of simulated Higgs signal and $Z^0 \to \tau^+\tau^-$ background.

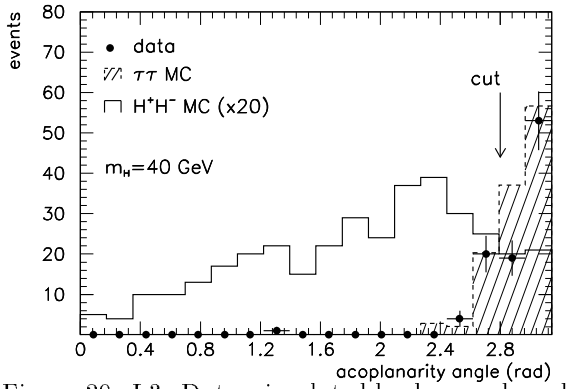

Figure 29. L3: Data, simulated background, and a 40 GeV $\tau\nu\tau\nu$ Higgs signal.

No indication of a charged Higgs has been observed, and mass limits as a function of the charged Higgs decay branching ratio have been set by all LEP experiments.

4. Interpretation in the 2-Doublet Model

Production rates for Higgs boson bremsstrahlung and neutral Higgs boson pair-production are complementary. Therefore, a Higgs boson cannot escape detection if it is kinematically accessible. The search for Higgs bremsstrahlung in the MSM Higgs decay channels with reduced production rates is particularly important. The experimental results set limits on the parameters of the general two-doublet model.

4.1. Non-Minimal Neutral Higgs Bosons

Curve (A) in Fig. 19 (from [14]) can be interpreted as a limit on the parameter $\sin^2(\beta-\alpha)$ of the two-doublet model.

The value $\cos^2(\beta-\alpha)$ can be constrained by the precision Z-lineshape measurements owing to the large production rate of $Z^0 \to h^0A^0$. Any non-minimal MSM contribution to the Z-width larger than 32 MeV is excluded at 95% CL [20]. The production rate of $Z^0 \to h^0A^0$ depends on the Higgs masses and the $\cos^2(\beta-\alpha)$ value. A limit on $\cos^2(\beta-\alpha)$ is shown in Fig. 30 (from [15]). Most important is the combination of sine and cosine limits as presented in Fig. 31 (from [15]).

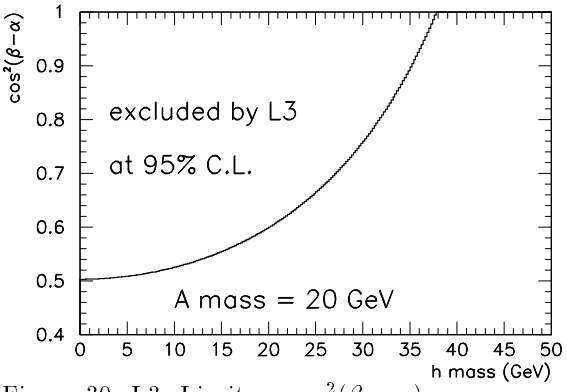

Figure 30. L3: Limit on $\cos^2(\beta-\alpha)$.

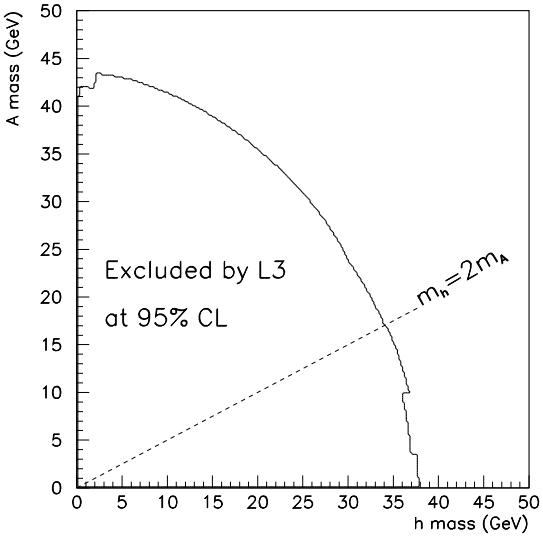

Figure 31. L3: Limits on (m_h,m_A).

In addition to the limits on $\cos^2(\beta-\alpha)$ from the Z-lineshape, direct searches can be included under assumptions on the Higgs branching ratios, which are functions of α and $\tan\beta$. Limits in the ($m_{\rm h}$,$m_{\rm A}$) plane are shown in Fig. 32 (from [21]).

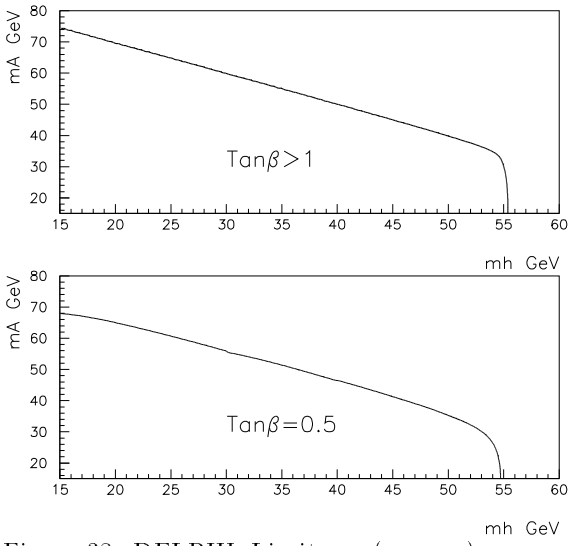

Figure 32. DELPHI: Limits on ($m_{\rm h}$,$m_{\rm A}$).

4.2. Non-Minimal Charged Higgs Bosons

In the two-doublet model the charged Higgs boson production rate is only a function of the charged Higgs mass [22]. The number of expected events is shown in Fig. 33 for 1 million hadronic Z decays.

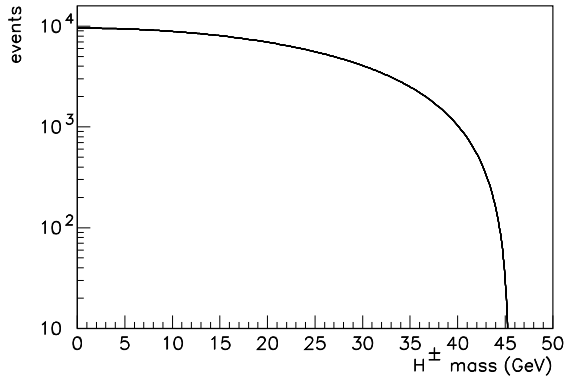

Figure 33. Charged Higgs production rates.

The three important charged Higgs decay channels, cscs, cs$\tau\nu$, and $\tau\nu\tau\nu$, are combined and lead to a decay mode independent exclusion of a charged Higgs boson, as shown in Fig. 34 (from [15]). The combined limits of the four LEP experiments lead to an exclusion of charged Higgs boson with masses near the kinematic production limit of about 45 GeV [23,21,15,24].

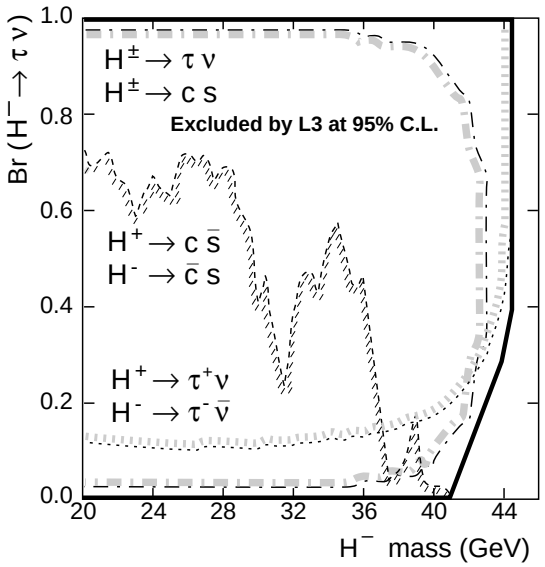

Figure 34. L3: Charged Higgs mass limits from direct searches.

A strong limit on the charged Higgs boson mass can result from the CLEO measurement of BR(b $\rightarrow$ sγ) $< 5.4\times10^{-4}$ [25]. Using calculations of the charged Higgs contribution to this decay rate [26,27], a charged Higgs boson with $m_{\rm H^\pm} < 260$ GeV is excluded independent of the $\tan\beta$ value, as shown in Fig. 35. However, this limit is very top-mass dependent, and it can vanish completely [28] if Supersymmetric particles cancel the charged Higgs contribution to the branching fraction.

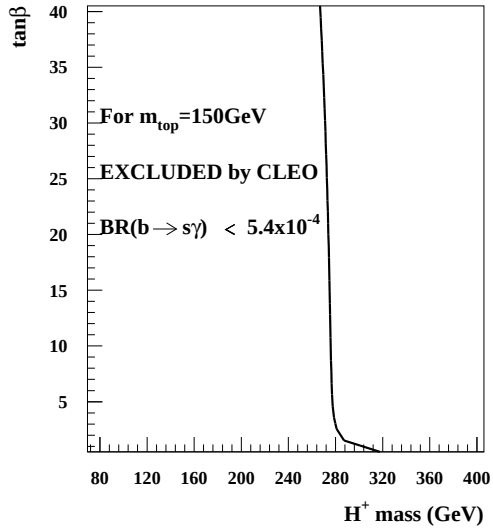

Figure 35. Charged Higgs boson mass limits from $b \to s\gamma$ constraints.

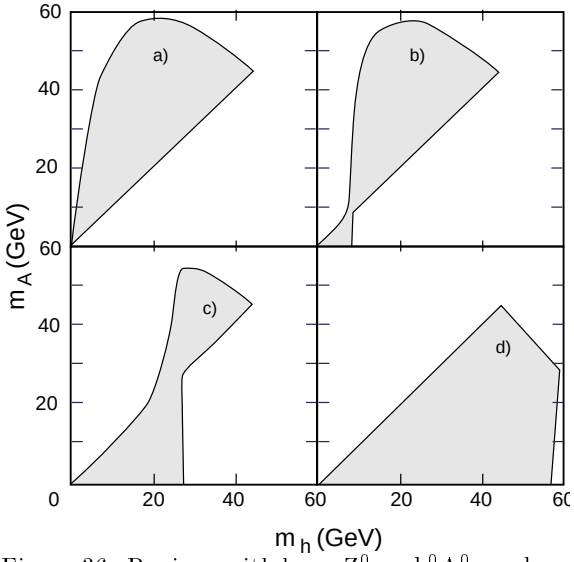

Figure 36. Regions with large $Z^0 \to h^0A^0$ production depending on the amount of radiative corrections in the MSSM.

Beyond the framework of the two-doublet model, doubly charged Higgs bosons have been searched for, as predicted in triplet models. They are excluded in almost the entire parameter space up to their kinematic production limit of about 45 GeV [29].

5. Interpretation in the MSSM

The MSSM [30] Higgs boson production rates and decay branching ratios are functions of the Higgs boson masses. When important radiative corrections to the tree-level calculations are included, the production rates and decay branching fractions will also depend on a large number of unknown parameters of the Supersymmetric model. In good approximation all experiments interpret their results as a function of top and stop masses. The effect of radiative corrections is illustrated in Fig. 36 (from [16]). The regions are shown where more than 250 $Z^0 \to h^0A^0$ events per 1 million hadronic Z decays are expected for a) no radiative corrections, up to d) large radiative corrections (m_t = 200 GeV and $m_{\tilde{t}}$ = 1 TeV). Compared to the tree-level calculations, Fig. 36 a), the (m_h,m_A) parameter space is largely extended.

Figure 37 (from [14,11,15,19]) shows the MSSM results of the four LEP experiments for independent variation over top and stop masses (except DELPHI, which has fixed top and stop masses).

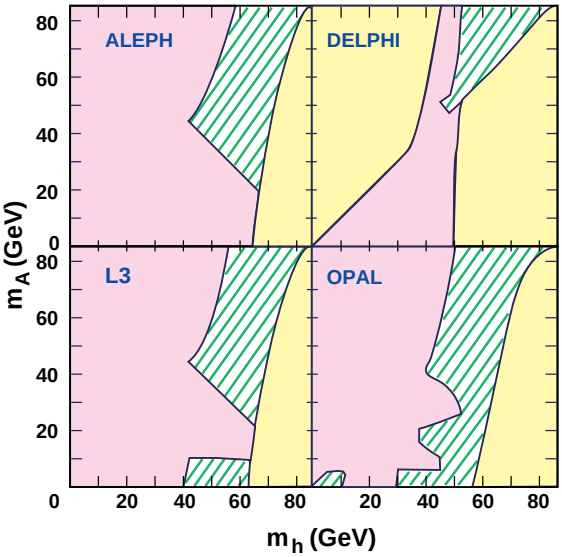

Figure 37. ALEPH, DELPHI, L3, OPAL: MSSM results on reduced data sets. The dark region is excluded, the hatched region allowed, and the light region not allowed by the theory.

6. Prospects of Higgs Searches at LEP2

The physics potential for minimal and non-minimal Higgs searches has been studied for center-of-mass energies of 175, 190, and 210 GeV. According to the planning for LEP2 [31], it will be possible to obtain a center-of-mass energy of about 175 GeV. This corresponds to the installation of 196 approved cavities with an acceleration gradient of 6 MV/m. At a later stage, the installation of 256 cavities would increase the center-of-mass energy to 190 GeV. The installation of 384 cavities would further increase the energy to 210 GeV. The ultimate energy limit of the LEP programme, of about 240 GeV, which is set by the maximal bending power of the magnets, could eventually be achieved with additional or better performing cavities. The aim is to reach the W^+W^- threshold in 1996 [32].

The method of search developed at LEP1 will be fully applicable at LEP2; in addition, new techniques for b-tagging and invariant jet mass reconstructions will be important to cope with the $e^+e^- \to W^+W^-$ background production. Figure 38 shows diagrams of background reactions and their expected cross sections for $\sqrt{s} = 190$ GeV. All processes have been simulated with PYTHIA [33], except $e^+e^-f^+f^-$ which has been simulated with DIAG36 [34]. A fast, but realistic, detector simulation has been performed. Details of the simulations and the event selections are given in [35] for $\sqrt{s} = 175$, 190, and 210 GeV.

Unlike at LEP1 the 4-jet channel ($H^0Z^0 \to b\bar{b}q\bar{q}$) can also be used in the MSM Higgs search at LEP2 due to the much-suppressed background from hadronic Z decays. New sources of 4-jet background will arise from $W^+W^- \to q\bar{q}q\bar{q}$ and $Z^0Z^0 \to q\bar{q}q\bar{q}$.

In addition, W^+W^- decays will lead to the same final states as expected from charged Higgs decays. Branching ratios are listed in Table 3.

Table 3
WW and ZZ decay branching ratios.

WW Decay	BR(%)	ZZ Decay	BR(%)
$\tau^+\nu\tau^-\bar{\nu}$	1.1	$b\bar{b}b\bar{b}$	2.3
$q\bar{q}\ \tau\nu$	14	$c\bar{c}b\bar{b}$	4.0
$q\bar{q}q\bar{q}$	47	$c\bar{c}c\bar{c}$	1.7
		$q\bar{q}q\bar{q}$	49

6.1. MSM Higgs Boson

All LEP experiments can obtain approximately the same sensitivity for the MSM Higgs boson. A selection sensitivity of about 0.05 to 0.15 pb with $\mathcal{L} = 500\ \mathrm{pb}^{-1}$ for a 3σ effect of signal to background ratio ($\sigma = \mathrm{signal}/\sqrt{\mathrm{background}}$) can be achieved over the Higgs mass range from 70 to 120 GeV depending on $\sqrt{s}$ [36]. The sensitivity in the mass range between 90 and 110 GeV is slightly weaker due to the irreducible background from $e^+e^- \to Z^0Z^0$ events.

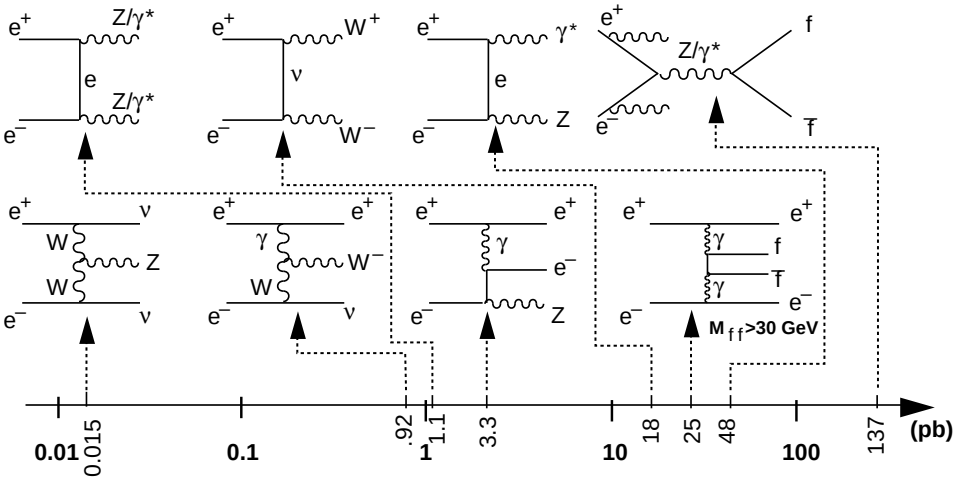

Figure 38. LEP2 background reactions and cross sections for $\sqrt{s} = 190$ GeV.

Therefore, more generally, any bremsstrahlung-produced Higgs boson in a non-minimal SM with decay branching ratios similar to those expected for the MSM Higgs boson would be discovered if

$$\sigma(e^+e^- \to h^0 Z^0) \geq 0.2 \text{ pb}. \quad (1)$$

In the MSM, the expected Higgs boson cross section is well known as a function of its mass, and its discovery limit at LEP2 can be expressed in good approximation as a function of $\sqrt{s}$:

$$m_{H_{MSM}}^{limit} = \sqrt{s} - m_Z \quad (\pm 5 \text{ GeV}), \quad (2)$$

where the positive sign is valid for a center-of-mass energy near the W^+W^- threshold and the negative sign for a center-of-mass energy around 210 GeV. The cross section for the MSM Higgs boson as a function of the center-of-mass energy is shown in Fig. 39 (from [35]).

The minimum luminosity needed for a Higgs boson discovery as a function of the Higgs boson mass is shown in Fig. 40 (from [37]) for $\sqrt{s} =$ 175 GeV. A Higgs boson with a mass of about 80 GeV would be detectable with a 5σ effect for $\mathcal{L} = 500$ pb^{-1}.

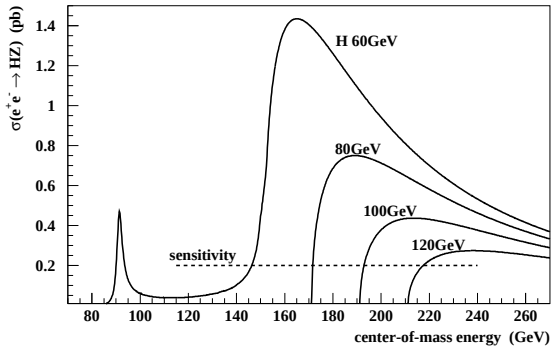

Figure 39. MSM Higgs cross sections and experimental sensitivity.

Figure 41 (from [35]) shows the L3 limit [15] and an extension of the $\sin^2(\beta-\alpha)$ sensitivity range as a function of the Higgs mass at $\sqrt{s} =$ 210 GeV with a detection sensitivity of 0.2 pb. A sufficient overlap with the current limits is achieved when a selection sensitivity of 0.2 pb can be maintained also for a 30 GeV Higgs boson. A similar extension has been reported in Ref. [38].

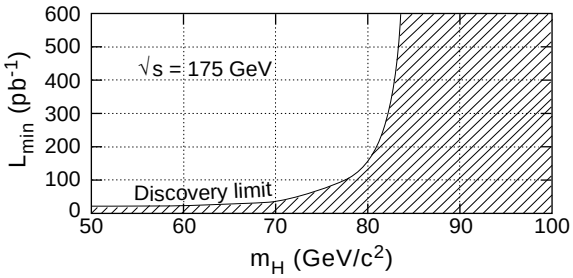

Figure 40. Minimum luminosity needed to discover the MSM Higgs bosons with a 5σ effect.

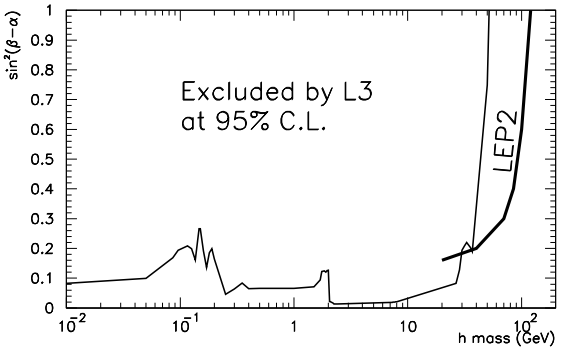

Figure 41. Limit on $\sin^2(\beta-\alpha)$ from L3 and sensitivity extension for LEP2 with $\sqrt{s} = 210$ GeV and $\mathcal{L} = 500$ pb^{-1}.

6.2. Non-Minimal Neutral Higgs Bosons

Already in the first phase of LEP2, a significant increase of the mass parameter space compared to LEP1 for a discovery of non-minimal Higgs bosons will be possible as shown in Fig. 42. Figure 43 (from [35]) illustrates the effect of b-jet tagging in the $e^+e^- \to h^0A^0 \to b\bar{b}b\bar{b}$ search. The simulated effects of b-tagging on signal efficiency and background rejection are listed in Table 4 (from [35]) for an example of $m_h = 60$ GeV and $m_A = 100$ GeV at $\sqrt{s} = 210$ GeV, applying a simple b-tagging algorithm [39,40].

Table 4
b-tagging efficiency and background rejection.

Eff. (in %)	Rejection Power (in %)			
$b\bar{b}b\bar{b}$	$q\bar{q}$	γZ^0	W^+W^-	Z^0Z^0
60	31	36	105	11

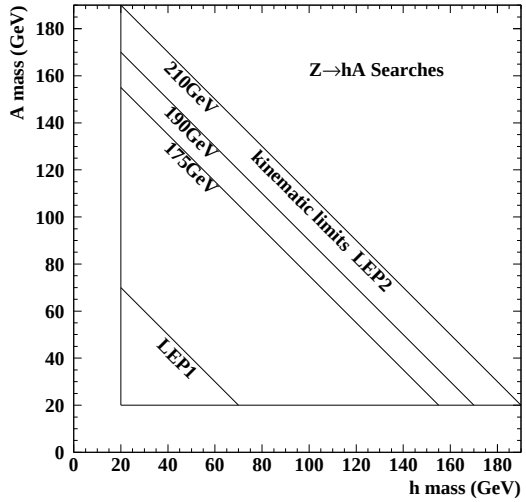

Figure 42. Kinematically accessible regions for Higgs boson pair-production at LEP1 and LEP2.

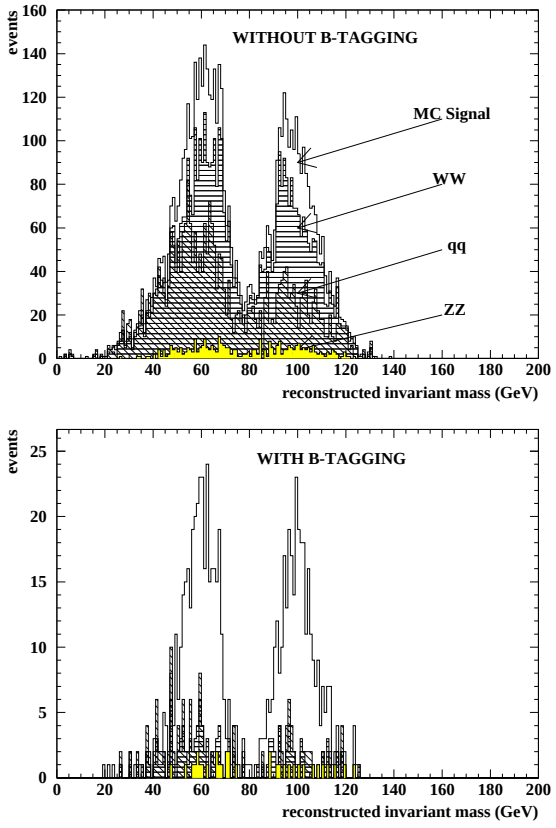

Figure 43. Simulated Higgs bosons and background: b-tagging is required for signal sensitivity ($\sqrt{s} = 210$ GeV, $\mathcal{L} = 500$ pb^{-1}).

Higgs boson mass resolutions of about 10% and a 3σ detection sensitivity of 0.12 pb have been obtained in this simulation. The sensitivities vary much as a function of ($m_{\rm h}$,$m_{\rm A}$) [35]. Based on the experience acquired at LEP1, larger sensitivities are expected for the $\tau\tau$bb and $\tau\tau\tau\tau$ channels.

6.3. On a Decisive Test of the MSSM

The upper mass on $m_{\rm h}$ is shown in Fig. 44 (from [41]) as a function of various parameters of the Supersymmetric model and for two top masses. For a top mass of 180 GeV [2] the upper bound on $m_{\rm h}$ is 137 GeV.

Owing to the complementary character of Higgs bremsstrahlung and Higgs pair-production, a decisive test of the MSSM will require simultaneous searches. The parameter regions in which a Higgs signal can be discovered for $\sqrt{s} =$ 210 GeV and $\mathcal{L} = 500$ pb^{-1} are shown in Fig. 45 (from [43]). Four regions can be distinguished for $113 \leq m_{\rm t} \leq 180$ GeV and $\tan\beta \geq 0.5$:

(A) The sensitivity region.
(B) The region, where sensitivity depends on the choice of Supersymmetric parameters.
(C) The non-sensitivity region.
(D) The region not allowed in the MSSM.

A substantial region (B) reflects a dependence of the discovery potential on the choice of Supersymmetric parameters.

6.4. Non-Minimal Charged Higgs Bosons

A discovery of a charged Higgs boson would be unambiguous evidence of physics beyond the MSM, and even beyond the MSSM if $m_{\rm H^\pm} < m_{\rm Z}$. The charged Higgs production rate [22] for $\mathcal{L} =$ 500 pb^{-1} is illustrated in Fig. 46 (from [35]) for $\sqrt{s} =$ 175, 190 and 210 GeV.

In the cscs channel a mass resolution of about 1 GeV can be obtained, as shown in Fig. 47 (from [35]). In addition to the selection for a cs$\tau\nu$ signal at LEP1, the reconstruction of the invariant mass of the $\tau\nu$ system can also be used to discriminate against $\rm W^+W^- \to c\bar{s}\tau^-\nu$ background, as shown in Fig. 48 (from [35]). In the $\tau\nu\tau\nu$ channel, leptonic $\rm W^+W^-$ decays can largely be rejected by the reconstruction of the visible τ energies, as shown in Fig. 49 (from [35]).

[2] Recently the CDF Collaboration reported evidence for the top quark with $m_{\rm t} = 174 \pm 10^{+13}_{-12}$ [42].

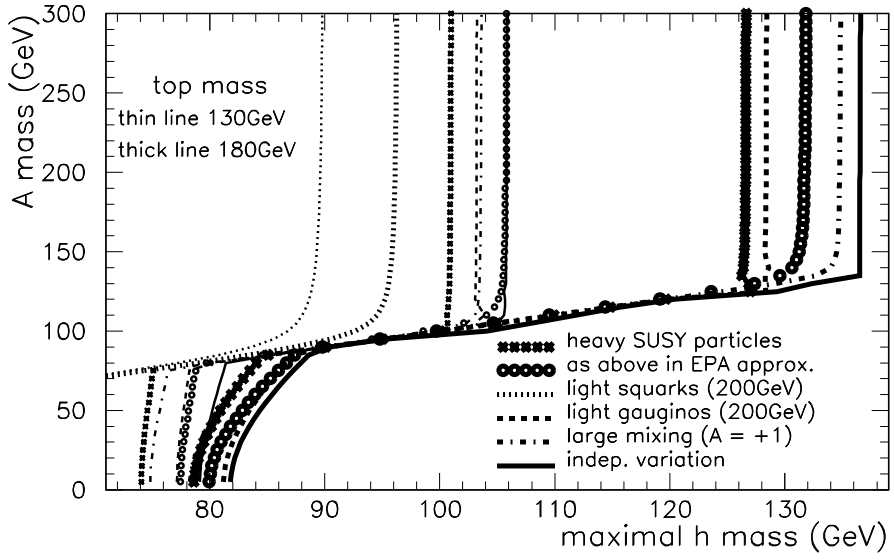

Figure 44. Upper bound on the h^0 mass depending on parameters in the MSSM.

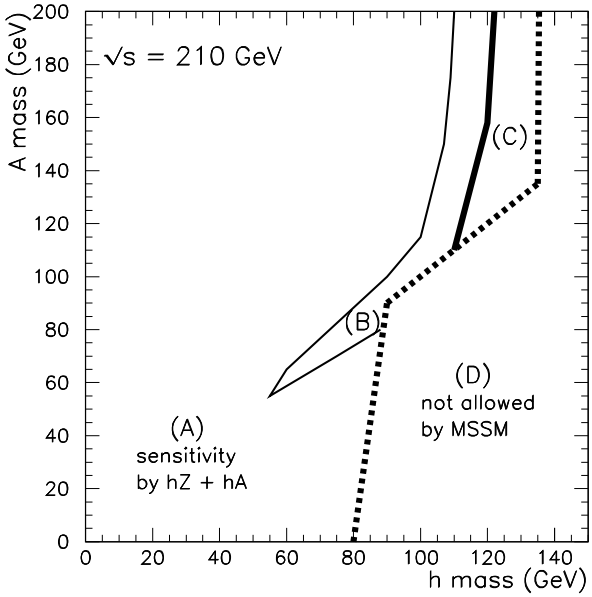

Figure 45. Accessible MSSM ($m_{\rm h}$,$m_{\rm A}$) regions.

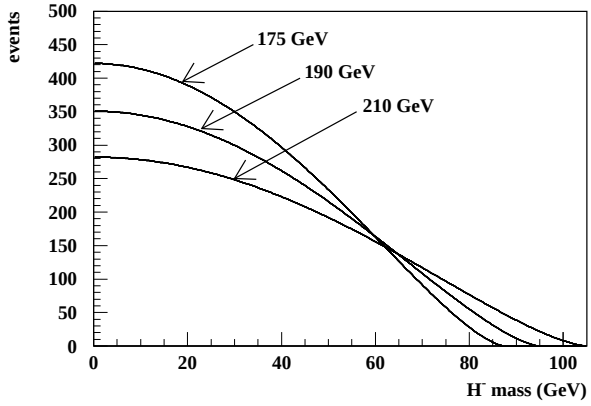

Figure 46. Number of charged Higgs bosons expected for $\sqrt{s} = 175, 190$, and 210 GeV.

Figure 50 (from [35]) shows the combined reach of the three search channels. A signal would be visible up to $m_{\rm H^{\pm}} \approx 70$ GeV. A large total luminosity is crucial for a significant extension of the charged Higgs boson discovery potential beyond the LEP1 limit due to the small variation of the event rate with the center-of-mass energy and the rather small number of expected events at LEP2.

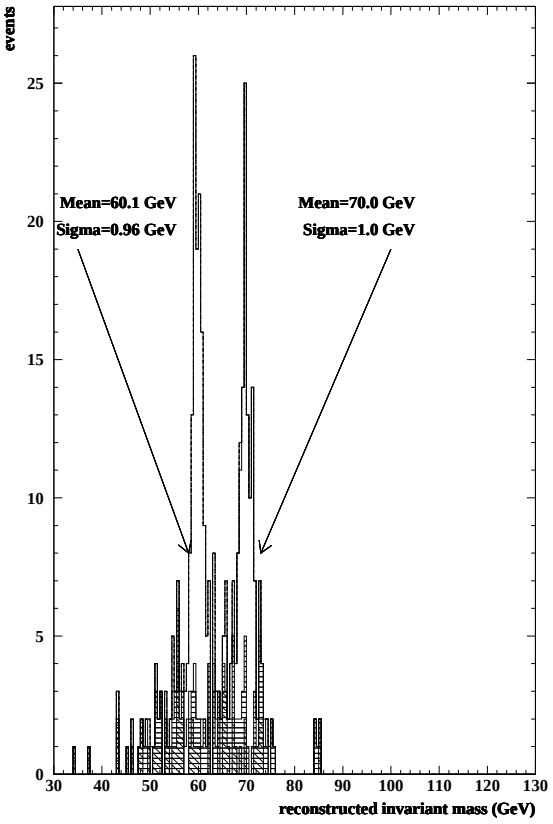

Figure 47. Simulated 60 and 70 GeV charged Higgs bosons and background in the cscs channel.

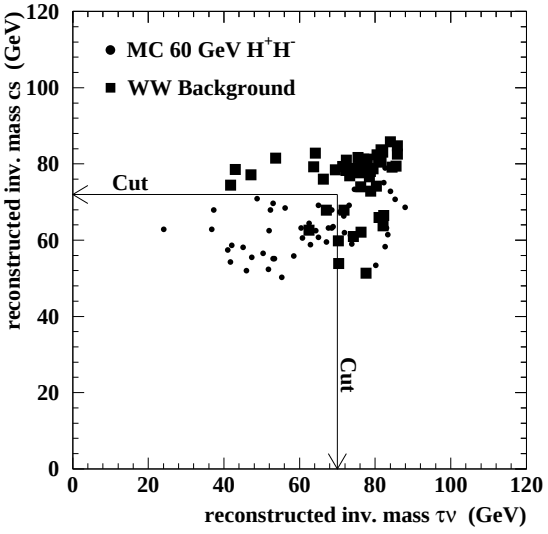

Figure 48. Reconstruction of M_{cs} and $M_{\tau\nu}$.

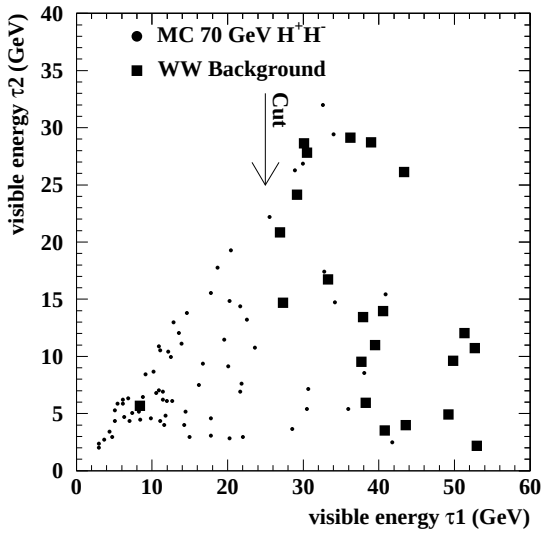

Figure 49. Final selection in the $\tau\nu\tau\nu$ channel.

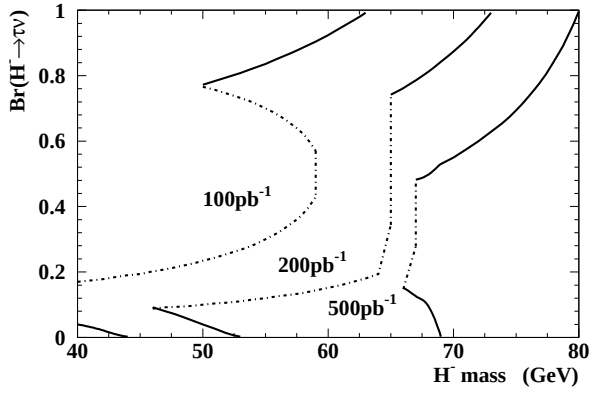

Figure 50. Sensitivity regions for $\sqrt{s} \approx 200$ GeV and $\mathcal{L} = 100$, 200, and 500 pb^{-1}.

7. Conclusions

The search for the Higgs boson of the MSM has exceeded expectations. The pre-LEP expectations for the sensitivity range of LEP1 were about 30 GeV [4], while a Higgs mass larger than 60 GeV has been excluded. In first approximation the combined limit from the LEP experiments on the MSM Higgs boson mass is 63.5 GeV at 95% CL. The observation of further irreducible background from 4-fermion processes could slightly decrease the Higgs mass limit. At LEP1 the MSM Higgs boson sensitivity approaches its saturation. Only a small sensitivity increase, up to about 65 to 70 GeV, can be expected with 10 million hadronic Z decays.

In the two-doublet Higgs model, searches for neutral and charged Higgs bosons lead to various limits on their production rates. Charged Higgs bosons are excluded independently of the decay mode up to the kinematic reach of LEP1 of about 45 GeV. Mass limits and limits on $\sin^2(\beta-\alpha)$ and $\cos^2(\beta-\alpha)$ are obtained. Additional LEP1 data will be important to establish higher sensitivities for Higgs bremsstrahlung production and neutral Higgs pair-production, since both production rates are unpredicted. In the MSSM, LEP1 has almost covered the kinematically accessible parameter mass region and excluded it.

The prospects of the Higgs search at LEP2 will predominantly depend on the achievable center-of-mass energy and the total integrated luminosity. The MSM Higgs boson reach will be from 80 to 110 GeV for about $\sqrt{s} = 170$ to 210 GeV. Already in the first phase of LEP2, a significant increase of the mass parameter space compared to LEP1 for a discovery of non-minimal Higgs bosons will be possible, while the mass range for a discovery of the minimal Standard Model Higgs boson will increase only marginally. With a large center-of-mass energy almost the entire allowed ($m_{\rm h}$,$m_{\rm A}$) parameter space of the MSSM will be accessible. A decisive test of the MSSM depends on the values of top mass and Supersymmetric parameters. The sensitivity mass range for a charged Higgs boson will be about 70 GeV for $\mathcal{L} = 500$ pb^{-1} depending largely on the total integrated luminosity.

8. Acknowledgements

I would like to thank my fellow Higgs hunters for many fruitful discussions: J.-F. Grivaz, P. Janot (ALEPH), G. Crosetti, F. Richard (DELPHI), E. Duchovni, E. Gross, P. Sherwood (OPAL), J. Alcaraz, V. Andreev, L. Barone, M. Felcini, E. Fiandrini, A. Gurtu, G. Coignet, A. Kunin, P. Lebrun, E. Leonardi, B. Lindemann, L. Lista, J.-P. Martin, B. Monteleoni, S. Paoletti, F. Pauss, P. Razis, M. Pieri, B. Zhou (L3). I also wish to express my gratitude for the hospitality at the Lisbon Fall School to P. Abreu, G. Branco, and M. Pimenta.

REFERENCES

1. P.W. Higgs, *Phys. Lett.* **12** (1964) 132;
   P.W. Higgs, *Phys. Rev. Lett.* **13** (1964) 508;
   P.W. Higgs, *Phys. Rev.* **145** (1966) 1156;
   F. Englert and R. Brout, *Phys. Rev. Lett.* **13** (1964) 321;
   G.S. Guralnik, C.S. Hagen and T.W.B. Kibble, *Phys. Rev. Lett.* **13** (1964) 585.
2. S.L. Glashow, *Nucl. Phys.* **22** (1961) 579;
   A. Salam, *Phys. Rev.* **127** (1962) 331;
   A. Salam, in: "Elementary Particle Theory", ed. N. Svartholm (Stockholm, 1968), p. 361;
   S. Weinberg, *Phys. Rev. Lett.* **19** (1967) 1264.
3. G. Altarelli, R. Barbieri, and F. Caravaglios, Preprint CERN, TH/6859-93 (1993).
4. S. Dawson, J.F. Gunion, H.E. Haber and G.L. Kane, "The Physics of the Higgs Bosons: Higgs Hunter's Guide" (Addison Wesley, Menlo Park, 1989).
5. F. A. Berends and R. Kleiss, *Nucl. Phys.* **B 260** (1985) 32.
6. B.L. Ioffe and V.A. Khoze, Preprint LINP, Leningrad, Nov. 1976;
   J.D. Bjorken, Proc. of the 1976 SLAC Summer Institute on Particle Physics, Stanford, ed. M.C. Zipf (SLAC, Stanford, 1977) p. 1.
7. B.A. Kniehl, *Z. Phys.* **55** (1992) 605,
   A. Denner *et al.*, *Z. Phys.* **56** (1992) 261.
8. P.J. Franzini *et al.* in "Z Physics at LEP 1", eds. G. Altarelli, R. Kleiss and C. Verzegnassi, CERN Report CERN-89-08, Vol. 2 (1989) p. 59.

9. DELPHI Collaboration, P. Abreu *et al.*, *Nucl. Phys.* **B 342** (1990) 1.
10. ALEPH Collaboration, D. Buskulic *et al.*, *Phys. Lett.* **B 313** (1993) 299; Physics notes 94-28, 94-29, and 94-30, March 1994.
11. DELPHI Collaboration, P. Abreu *et al.*, *Nucl. Phys.* **B 373** (1992) 3; Preprint CERN, PPE/94-46 Rev (1994).
12. L3 Collaboration, *Phys. Lett.* **B 303** (1993) 391.
13. OPAL Collaboration, M.Z. Akrawy *et al.*, *Phys. Lett.* **B 253** (1991) 511; Preprint CERN, PPE/94-48 (1994).
14. ALEPH Collaboration, D. Buskulic *et al.*, *Phys. Lett.* **B 313** (1993) 312.
15. L3 Collaboration, O. Adriani *et al.*, *Z. Phys.* **C 57** (1993) 355.
16. A. Sopczak, "Search for Non-minimal Higgs Bosons from Z^0 Decays with the L3 Experiment at LEP", Ph.D. Thesis, U. of Cal., San Diego, 1992.
17. L3 Collaboration, B. Adeva *et al.*, *Phys. Rep.* **236** (1993) 1.
18. DELPHI Collaboration, DELPHI 93-102 PHYS 329, contributed paper to the International Europhysics Conference on High Energy Physics, Marseille, 22-28 July, 1993.
19. OPAL Collaboration, P.D. Acton *et al.*, *Phys. Lett.* **B 265** (1991) 475.
20. A. Sopczak, L3 Note #1372, "Limits on Physics Beyond the Minimal Standard Model from LEP Line-Shape Data", March 1993.
21. DELPHI Collaboration, P. Abreu *et al.*, DELPHI Note 92-75, 1992.
22. S. Komamiya, *Phys. Rev.* **D 38** (1988) 2158.
23. ALEPH Collaboration, D. Decamp *et al.*, *Phys. Lett.* **B 241** (1990) 623.
24. OPAL Collaborations, M.Z. Akrawy *et al.*, *Phys. Lett.* **B 242** (1990) 299.
25. CLEO Collaboration, E. Thorndike *et al.*, CLEO Preprint, CLN93/1212, CLEO93-06.
26. J.L. Hewlett, *Phys. Rev. Lett.* **70** (1993) 1045.
27. V. Barger, M.S. Berger and R.J. Phillips, *Phys. Rev. Lett.* **70** (1993) 1368.
28. F.M. Borzumati, Preprint DESY 93-090, 1993.
29. OPAL Collaboration, M.Z. Akrawy *et al.*, *Phys. Lett.* **B 295** (1992) 347.
30. Y.A. Golfand and E.P. Likhtman, *JETP Lett.* **13** (1971) 323;
    D.V. Volkhov and V.P. Akulov, *Phys. Lett.* **B 46** (1973) 109;
    J. Wess and B. Zumino, *Nucl. Phys.* **B 70** (1974) 39;
    P. Fayet and S. Ferrara, *Phys. Rep.* **32** (1977) 249;
    A. Salam and J. Strathdee, *Fortschr. Phys.* **26** (1978) 57;
    H.P. Nilles, *Phys. Rep.* **110** (1984) 1.
31. C. Rubbia, Proc. LP-HEP 1991, Geneva, (World Scientific, Singapore, 1991) p.441.
32. C. Wyss, LEPC Meeting, CERN, LEPC/94-6, February 1994.
33. T. Sjöstrand, Preprint CERN-TH., 6488/92 (1992).
34. F. A. Berends, P. H. Daverveldt and R. Kleiss, *Nucl. Phys.* **B 253** (1985) 441.
35. A. Sopczak, Int. J. Mod. Phys. **A9** (1994) 1747.
36. D. Treille, Review talk given at the LEPC Meeting, CERN, November 3, 1992.
37. P. Janot, Proc. XIII Moriond Workshop, 1992, France (Ed. Frontieres, 1993) p.317.
38. A. Lopez-Fernandez, J.C. Romao, F. de Campos and J.W.F. Valle, *Phys. Lett.* **B 312** (1993) 240.
39. B. Zhou, 'Study of b-tagging for LEP200', Internal Report, Boston University, Oct. 29, 1992.
40. J. Alcaraz *et al.*, Preprint CERN, PPE/93-28 (1993).
41. J. Rosiek, A. Sopczak, P. Chankowski, and St. Pokorski, Preprint CERN, PPE/93-198 (1993).
42. CDF Collaboration, F. Abe *et al.*, FERMILAB, PUB-94/097-E.
43. J. Rosiek and A. Sopczak, Proc. Int. School on Cosmological Dark Matter, Valencia, Spain, October 4-8,1993 (in the press).